

A Zero-Dimensional Model of a 2nd Generation Planar SOFC Using Calibrated Parameters

Thomas Frank Petersen*

Risø National Laboratory, Materials Research Department, PhD Student
Frederiksborgvej 399, P.O. 49, DK-4000 Roskilde.
E-Mail: thomas.frank.petersen@risoe.dk

Associate Professor Niels Houbak and Associate Professor Brian Elmegaard
Technical University of Denmark
Department of Mechanical Engineering, DK-2800 Lyngby

Abstract

This paper presents a zero-dimensional mathematical model of a planar 2nd generation co-flow SOFC developed for simulation of power systems. The model accounts for the electrochemical oxidation of hydrogen as well as the methane reforming reaction and the water-gas shift reaction. An important part of the paper is the electrochemical sub-model, where experimental data was used to calibrate specific parameters. The SOFC model was implemented in the DNA simulation software which is designed for energy system simulation. The result is an accurate and flexible tool suitable for simulation of many different SOFC-based power systems.

Keywords: Solid oxide fuel cells, SOFC, mathematical modelling.

1. Introduction

The Solid Oxide Fuel Cell (SOFC) is one of the most promising types of fuel cells because of the potential for a high electrical efficiency and low environmental impact. The SOFC has a high operating temperature and can, in addition to hydrogen, use hydrocarbons like methane and natural gas directly as fuels. The high temperature makes the SOFC a candidate for small energy systems like cogeneration systems or hybrid systems where the high quality heat rejected by the SOFC is utilized in secondary heat engines to increase the power production. However, SOFC energy systems are complex and a flexible simulation tool is required to analyze the systems in detail. This paper presents a steady-state model of a planar co-flow SOFC for system-level simulation. From a system perspective, the SOFC is only one component out of many where only the inlet and the outlet conditions are important. The modelling presented here is deliberately kept simple to ensure that the SOFC model is computationally fast to allow detailed parameter variations of multiple system operating parameters. The electrochemical model used here is well-

established in previous works, see e.g. (Costamagna et al., 2001) or (Massardo and Lubelli, 2000). However, the present work improves the existing models by using experimental data to calibrate specific parameters of the generic theoretical model. Some of the parameters in question have previously been assumed constant due to a lack of empirical data, but here it is demonstrated how the parameters can be extracted from experimental data. The result of the calibration is an increase of the accuracy of the generic electrochemical models. It should be noted that since this paper was written, other papers have been published with more detailed electrochemical models than the one used here. State-of-the-art SOFC models can be found in for example (Costamagna et al., 2004) or (Bove et al., 2005). The presented SOFC model also incorporates a flexible chemical model based on the minimization of Gibbs energy. Currently, the chemical model only supports fuel mixtures consisting of H₂, CO and CH₄, but the generality of the chemical model allow it to be extended to any type of fuel mixture. This is an advantage in system simulation as SOFCs are expected to operate on a variety of fuels.

*Author to whom correspondence should be addressed

2. The DNA Simulation Tool

The mathematical SOFC model was implemented in the software package "Dynamic Network Analysis" (DNA). DNA is a component-based simulation tool designed for simulation of many types of energy systems developed at the Technical University of Denmark (Elmegaard 1999). DNA features:

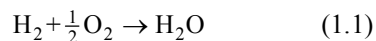
- A large component library of common energy system components.
- Calculation of all gas compositions.
- Built-in routines for thermodynamic, transport and radiative properties.
- Satisfaction of mass and energy conservation for all system components.

By implementing the SOFC model in DNA, the existing component library can be utilized in subsequent system simulation models. DNA is open source and can be downloaded from:

<http://www.et.mek.dtu.dk/English/Software.aspx>

3. Description of the SOFC

The SOFC is an electrochemical reactor that oxidizes hydrogen into water and releases electrical power and heat in the process:



The SOFC consists of three parts: the anode and the cathode which are separated by an electrolyte which contains oxide ions (O^{2-}). Hydrogen is supplied at the anode and reacts with the O^{2-} ions in the electrolyte to produce water and free electrons. The electrons are transported through an external circuit from the anode to the cathode to generate an electric current. Oxygen (air) is supplied at the cathode and reacts with the electrons from the anode to produce new O^{2-} ions which are transported into the electrolyte.

The planar SOFC design is shown in Figure 1.

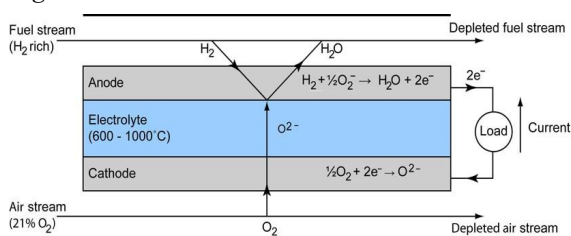
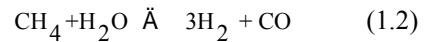


Figure 1. The planar SOFC design illustrated with electrochemical reactions.

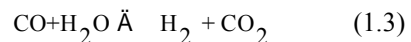
The voltage of a single SOFC is below one volt and to obtain higher voltages individual SOFCs are placed in stacks. Metallic interconnects, in the form of plates, are placed on both sides of the SOFCs to provide electrical

connection between the cells in the stack. Hydrogen and air are distributed to the surface of the cell through channels in the interconnects.

The SOFC requires a high operating temperature as the electrolyte is made from Yttria Stabilized Zirconia (YSZ) which only conducts ions above approximately 650°C . The high temperature allows methane to be used as a fuel through internal steam reforming (Larminie and Dicks, 2004):



In addition to the reforming reaction, hydrogen is produced by the water-gas shift reaction:



Both reactions (1.2) and (1.3) can be assumed to reach equilibrium quickly because of the high operating temperature and the high water vapor content. In addition, nickel is present in the anode which acts as a catalyst for both reactions (Larminie and Dicks, 2004). The equilibrium means that virtually all methane in the fuel can be assumed consumed within a few centimeters of the SOFC inlet (Henriksen, 2006). This assumption was verified in a previous study (Sorrentino et al., 2004). When carbon is present in the fuel, the Steam-To-Carbon-Ratio (STCR) must be above 2 to avoid carbon deposition which may destroy the anode (Braun, 2002). The STCR is defined as the molar ratio between water vapor and combustible components:

$$\text{STCR} = \frac{[\text{H}_2\text{O}]}{[\text{CH}_4] + [\text{CO}]} \quad (1.4)$$

Hydrogen and oxygen must be present at the SOFC exit to generate a usable voltage. The fuel utilization is defined as the ratio of hydrogen consumed to the total amount of hydrogen supplied (Braun, 2002):

$$U_f = \frac{\dot{n}_{\text{ox}}}{4\dot{n}_{\text{CH}_4} + \dot{n}_{\text{CO}_2} + \dot{n}_{\text{CO}}} \quad (1.5)$$

Equation (1.5) expresses methane and carbon monoxide as hydrogen equivalents; each methane molecule equals four hydrogen equivalents (three from the reforming reaction and one from the water-gas shift reaction) and each carbon monoxide molecule is equal to one hydrogen equivalent (from the water-gas shift reaction). Air supplies oxygen to the SOFC but also acts as a coolant. The flow of air is therefore many times greater than the flow of fuel.

4. The Mathematical SOFC Model

The zero-dimensional approach is used in the modelling which regards the SOFC as a

“black-box” and only determines the conditions at the boundaries of the SOFC. This approach is suitable for a model for system simulation, where only the outlet conditions and the electrical power produced are required outputs. The inputs to the model are:

1. The SOFC inlet conditions (temperature, pressure and gas concentrations).
2. The mass flow of inlet fuel.
3. The operating temperature of the SOFC.
4. The pressure loss over the SOFC.
5. The fuel utilization.

Furthermore, the geometry and materials used in the SOFC must be known, along with the total number of SOFCs and the number of SOFC stacks. The following assumptions are used for simplification of the SOFC model:

1. All species are considered ideal gases.
2. There is chemical equilibrium at the outlet of the SOFC.
3. The SOFC has a co-flow configuration (fuel and air flow in the same direction)
4. The fuel and air outlet temperatures are equal to the SOFC operating temperature (Iwata et al., 2000).
5. The anode and cathode are considered isopotential surfaces (Braun, 2002).
6. Single SOFC performance applies for the entire SOFC stack (Braun, 2002).

The governing equations of the SOFC model are split into the conservation equations and the constitutive equations. The conservation of mass and energy are formulated for a control volume on a molar basis, and the conservation of momentum can be reduced to a pressure balance (Braun, 2002). The pressure loss depends on the geometry of interconnect, and is regarded as an input parameter; it is normally in the order of 0.01 bar (Petersen, 2004). The constitutive equations are split into a sub-model of the chemical reactions occurring inside the SOFC and a sub-model of the electrochemical behavior of the SOFC. Only the constitutive equations are described here; for details on the conservation equations see (Petersen, 2004).

4.1 The Chemical Reaction Sub-Model

The chemical reaction sub-model evaluates the composition of the fuel and air exiting the SOFC and is based on chemical equilibrium and conservation of elements. To simulate both methane and hydrogen fueled SOFCs, both the steam reforming and the water-gas shift reactions are considered in addition to the electrochemical oxidation of hydrogen. For the fuel, the chemical

sub-model is based on the assumption of chemical equilibrium at the outlet of the SOFC. At the chemical equilibrium the Gibbs' free energy of any gas mixture reaches a minimum. Combined with the conservation of the atoms in the gas mixture, a system of equations can be formulated and solved to yield the concentration of each species at equilibrium. Using minimization of Gibbs energy to determine chemical equilibrium is described in further detail elsewhere (Elmegaard, 1999). Currently the model only determines the equilibrium for the species participating in reactions (1.1), (1.2) and (1.3), but may be extended to any fuel mixture. The amount of oxygen at the cathode outlet depends on the amount of oxidized hydrogen:

$$\left(\dot{n}_{\text{O}_2}^{\text{out}}\right)_{\text{ca}} = \left(\dot{n}_{\text{O}_2}^{\text{in}}\right)_{\text{ca}} - \frac{1}{2}\dot{i}_{\text{ox}} \quad (1.6)$$

Since the operating temperature of the SOFC is known, the total inlet and outlet flow of air is determined by the conservation equations.

4.2 The Electrochemical Sub-Model

The electrochemical sub-model evaluates the current-density, voltage and electrical power of the SOFC. The electrochemical behavior of a SOFC depends on the manufacture and the materials used. The electrochemical model presented here is based on general theoretical equations developed for planar 2nd generation SOFCs. The theoretical equations are subsequently calibrated using experimental data.

Faraday's Law states that the current-density (current per unit area of the SOFC) is directly proportional to the amount of reacting hydrogen:

$$\dot{i}_d = \frac{2 \cdot F \cdot \dot{i}_{\text{ox}}}{A} \quad (1.7)$$

The ideal potential between the anode and cathode is determined by the Nernst equation:

$$E_{\text{Nernst}} = -\frac{\Delta G^0}{2F} - \frac{RT}{2F} \cdot \ln \left(\frac{p_{\text{H}_2\text{O}}}{p_{\text{H}_2} \sqrt{p_{\text{O}_2}}} \right) \quad (1.8)$$

When current and power is drawn from the SOFC, the reactions in the fuel cell occur irreversibly. The result is polarizations which reduce the Nernst potential of the SOFC (Singhal and Kendall, 2003). There are three major types of polarizations: activation, Ohmic and concentration. A minor offset polarization, which is the result of contact resistance, internal current and leaks, also contributes to the total polarization. The SOFC operating voltage is found by subtracting the polarizations from the Nernst voltage:

$$E_{\text{SOFC}} = E_{\text{Nernst}} - \Delta V_{\text{act}} - \Delta V_{\text{Ohm}} - \Delta V_{\text{con}} - \Delta V_{\text{off}} \quad (1.9)$$

The overall operating voltage cannot exceed any local operating voltage because the electrodes are good electrical conductors and therefore isopotential (EG&G Technical Services, 2004). The SOFC will therefore adjust to the lowest local operating voltage. In a co-flow SOFC the lowest voltage occurs at the SOFC outlet, and Equation (1.9) is evaluated using the outlet conditions.

Activation polarization is the result of the energy requirements of the anode and the cathode to overcome the resistance to the transfer of electrons to and from the electrodes. Activation polarization dominates at low current-densities and is normally evaluated with the empirical and non-linear Butler-Volmer equation. However, in a SOFC the activation polarization is close to linear and is here evaluated with an approximation (Keegan et al., 2002):

$$\Delta V_{\text{act}} = \frac{RT}{\alpha F} \sinh^{-1} \left(\frac{i_d}{2i_0} \right) \quad (1.10)$$

Here α is the charge transfer coefficient and i_0 is the exchange current-density; both are determined by calibration.

The Ohmic polarization is described by Ohm's Law and depends on the electrical conductance of the electrodes and the ionic conductance of the electrolyte. The contribution from the metallic interconnect is neglected since its conductance is large compared to the other parts.

$$\Delta V_{\text{Ohm}} = \left(\frac{I_{\text{an}}}{\sigma_{\text{an}}} + \frac{I_{\text{ca}}}{\sigma_{\text{ca}}} + \frac{I_{\text{el}}}{\sigma_{\text{el}}} \right) \cdot i_d \quad (1.11)$$

The conductivities of the anode, cathode and electrolyte are evaluated with reference expressions developed for 2nd generation SOFCs (Chick et al., 2003). The anode is made of a composite of nickel and YSZ, where the conductance is assumed constant:

$$\sigma_{\text{an}} = 10^5 (\Omega^{-1} \text{m}^{-1}) \quad (1.12)$$

The cathode is made from Strontium-doped Lanthanum Manganite (LSM), and the conductance can be calculated with an Arrhenius-type expression:

$$\sigma_{\text{ca}} = \frac{A_{\text{ca}}}{T} \cdot e^{\left(\frac{-B_{\text{ca}}}{k_{\text{ca}} T} \right)} \quad (1.13)$$

The conductance of both the anode and cathode is corrected to account for porosity:

$$\sigma_{\text{porous}} = \sigma_{\text{solid}} \cdot (1 - 1.8\varepsilon) \quad (1.14)$$

The conductance of the electrolyte is evaluated with a third-order polynomial:

$$\sigma_{\text{el}} = A_{\text{el}} \cdot \theta^3 + B_{\text{el}} \cdot \theta^2 + C_{\text{el}} \cdot \theta + D_{\text{el}} \quad (1.15)$$

Here θ is the outlet temperature from the SOFC in Celsius. TABLE I and TABLE III list the constants used in Equations (1.13) – (1.15).

TABLE I. CONSTANTS USED TO CALCULATE THE CONDUCTANCE OF THE CATHODE (Chick et al., 2003).

Constant	Value	Unit
A_{ca}	5.760E7	$(T\Omega^{-1}\text{m}^{-1})$
B_{ca}	0.117	(eV)
k_{ca}	8.617E-5	(eVK^{-1})

TABLE II. CONSTANTS USED TO CALCULATE THE CONDUCTANCE OF THE ELECTROLYTE (Chick et al., 2003).

Constant	Value	Unit
A_{el}	8.588E-8	$(T^{-3}\Omega^{-1}\text{m}^{-1})$
B_{e}	-1.101E-4	$(T^{-2}\Omega^{-1}\text{m}^{-1})$
C_{el}	4.679E-2	$(T^{-1}\Omega^{-1}\text{m}^{-1})$
D_{el}	-6.54	$(\Omega^{-1}\text{m}^{-1})$

The concentration polarization is the result of diffusion, of products and reactants, to and from the interface between the electrolyte and the anode/cathode. The diffusion is associated with a resistance, which results in a voltage drop. Concentration polarization is dominant at high current-densities where the diffusion is greatest. When the current-density reaches either the anode or the cathode limiting currents, an insufficient amount of reactants is transported to the electrodes and the operating voltage is reduced to zero (Singhal and Kendall, 2003). The two limiting currents are evaluated as:

$$i_{\text{an}} = \frac{2Fp_{\text{H}_2} D_{\text{an,eff}}}{RTl_{\text{an}}} \quad i_{\text{ca}} = \frac{2Fp_{\text{H}_2} D_{\text{ca,eff}}}{RTl_{\text{ca}}} \quad (1.16)$$

because the anode is much thicker than the cathode, $i_{\text{as}} \ll i_{\text{ca,s}}$, and the cathode limiting current is neglected (Braun, 2002). The effective binary diffusion coefficient is determined as:

$$D_{\text{an,eff}} = \frac{D_{\text{an,bin}} \varepsilon_{\text{an}}}{\tau_{\text{an}}} \quad (1.17)$$

The concentration polarization is evaluated as:

$$\Delta V_{\text{conc}} = -B \cdot \ln \left(1 - \frac{i_d}{i_{\text{as}}} \right) + B \cdot \ln \left(1 + \frac{p_{\text{H}_2} \cdot i_d}{p_{\text{H}_2\text{O}} \cdot i_{\text{as}}} \right) \quad (1.18)$$

Both B and $D_{\text{an,bin}}$ are determined by calibration.

4.3 Calibration of the Electrochemical Model

The offset polarization, α , i_0 , the B parameter and $D_{an,bin}$ are all unknown parameters which depend on the manufacture of a given SOFC. These parameters are normally regarded as constants and determined from various references like (Larminie and Dicks, 2004). However, in this paper the above parameters are regarded as phenomenological and determined from experimental data. Nine current-voltage curves were obtained to determine the four parameters. The data came from two experiments performed by the Pacific Northwest National Laboratory (PNNL) (Chick et al., 2003). The first experiment was performed with a constant fuel composition of 97% hydrogen and 3% water vapor, and temperatures in the range of 650°C to 800°C. The second experiment was performed at a constant temperature of 750°C, with a fuel composition containing from 10% to 97% hydrogen concentration, 3% water vapor concentration and nitrogen as the remainder. In both experiments the flow of fuel was 200 standard cubic centimeters per minute (scm) and the flow of air was 300 scm. The fuel utilization was kept low to achieve almost constant operating conditions over the cell area. The experiments are summarized in TABLE III.

TABLE III. TEMPERATURE AND HYDROGEN CONCENTRATION RANGES FOR THE PNNL EXPERIMENTS. A “+” INDICATES A PERFORMED EXPERIMENT.

T/y _{H2}	10%	24%	49%	73%	97%
650°C	-	-	-	-	+
700°C	-	-	-	-	+
750°C	+	+	+	+	+
800°C	-	-	-	-	+

The active area of the PNNL cell is 3.8cm²; but the parameters determined here are assumed area-independent. Physical data for the SOFC used in the experiments are shown in TABLE IV.

TABLE IV. PHYSICAL DATA OF THE SOFC USED IN THE PNNL EXPERIMENTS.

Part	Thickness (μm)	Porosity (%)	Tortuosity (-)
Anode	600	30	2.5
Cathode	50	30	2.5
Electrolyte	10	-	-

The anode is much thicker than the other parts because 2nd generation SOFCs use the anode to provide mechanical strength to the cell.

At zero current-density all polarizations are zero, except for the offset polarization, which is the difference between the measured operating voltage and the Nernst potential. The offset

polarization is determined for the nine current-voltage curves and the average is show below:

$$\Delta V_{\text{off}} = 0.06\text{V} \quad (1.19)$$

To calibrate the activation polarization, the data from the first experiment is used. Due to the high hydrogen concentration it can be assumed that concentration polarization is negligible (Larminie and Dicks, 2004). All contributions to the total polarization are then either Ohmic, activation or offset polarization. The offset polarization has been determined previously and the Ohmic polarization can be determined from Equations (1.11) – (1.15). The activation polarization is isolated from the total polarization, and curve fitted to Equation (1.10) where α and i_0 are the only unknown parameters. This results in four values of α and i_0 which are expressed as functions of temperature:

$$\alpha = 1.698 \cdot 10^{-3} \cdot T - 1.254 \quad (1.20)$$

$$i_0 = \beta(T) \cdot \exp\left(\frac{4.221 \cdot 10^3}{RT}\right) \quad (1.21)$$

Here $\beta(T)$ is a pre-exponential factor which is a linear function of the temperature:

$$b_{\text{exp}} = 7.822 \times T - 6.530 \times 10^3 \quad (1.22)$$

To calibrate the concentration polarization the data from the second experiment are used. First the concentration polarization is isolated from the total polarization using the previously developed expressions for the activation, Ohmic and offset polarizations. This results in four different concentration polarization curves. These curves are fitted to Equation (1.18) and Equation (1.23) where B and $D_{an,bin}$ are the only unknowns. This yields four values of the parameter B and $D_{an,bin}$, which are expressed as functions of the hydrogen concentration. The B parameter is an inverse linear function of the hydrogen concentration. The function is modified to account for temperature, by assuming a linear dependence on temperature (Larminie and Dicks, 2004):

$$B = (8.039 \cdot 10^{-3} \cdot y_{\text{H}_2}^{-1} - 7.272 \cdot 10^{-3}) \cdot \frac{T}{T_{\text{ref}}} \quad (1.24)$$

The fitted expression for $D_{an,bin}$ is:

$$D_{an,bin} = -4.107 \cdot 10^{-5} \cdot y_{\text{H}_2} + 8.704 \cdot 10^{-5} \quad (1.25)$$

Because the binary diffusion constant is regarded as phenomenological, it implicitly includes effects like Knudsen diffusion, and adsorption and desorption. The binary diffusion coefficient depends on both temperature and pressure. According to the Chapman-Enskog diffusion theory the diffusion coefficient is inversely proportional to the pressure and

proportional to $T^{7/4}$. This allows the diffusion coefficient to be approximated at arbitrary pressures and temperatures if the diffusion coefficient is known at a reference pressure and temperature (Lienhard IV and Lienhard V, 2004):

$$D_{\text{bin}}(P, T) \gg D_{\text{bin,ref}} \left(\frac{T}{T_{\text{ref}}} \right)^{7/4} \left(\frac{P_{\text{ref}}}{P} \right) \left(\frac{\dot{O}}{\dot{O}_{\text{ref}}} \right) \quad (1.26)$$

Here D_{ref} is given by Equation (1.25) and P_{ref} and T_{ref} are 1 atm. and 750°C respectively. The error associated with the above approximation was determined from the Chapman-Enskog theory to be no larger than 1.1% in the temperature range from 650°C to 800°C. Notice that the calibrated functions are only valid in the temperature range where supported by experimental data. Figure 2 shows different polarizations as a function of the current-density calculated by the calibrated electrochemical sub-model.

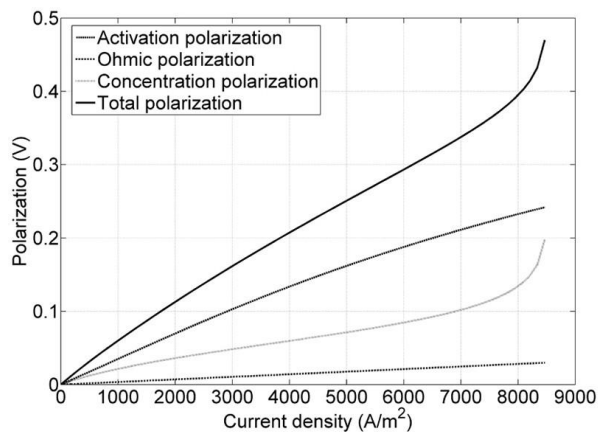


Figure 2. The activation, Ohmic and concentration polarizations at 750°C evaluated by the electrochemical model with a fuel composition of 24% H_2 , 3% H_2O and 63% N_2 .

For α equal to 0.5, Equation (1.10) is identical to the Butler-Volmer equation. However, Equation (1.20) shows that α lies between 0.31 and 0.57 in the temperature interval from 650°C to 800°C. To determine the effect of a non-constant value of α , Equation (1.10) was compared to the Butler-Volmer equation for current-densities between 1 and 20000. The two sets of activation polarization curves are in good agreement with correlation coefficients (R^2) ranging from 0.9995 at 650°C to 1.000 at 800°C. Since R^2 is very close to unity, it is concluded that Equation (1.10) gives a satisfactory representation of the activation polarization in the temperature range from 650°C to 800°C, even when α is different from 0.5.

4.4 Validation of the Electrochemical Sub-Model

The calibrated electrochemical sub-model is validated by comparing the predicted current-voltage curves to the experimental data. The comparison between the model and the first set of experimental data is shown in Figure 3 and shows a good agreement.

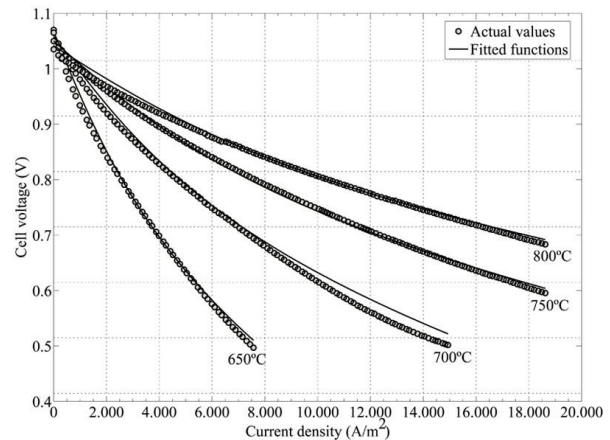


Figure 3. Comparison of experimental and model current voltage-curves from the first experiment. The lines are the model data and the circles are the experimental data.

The maximum difference between the model and the experimental curves occurs at 650°C with a correlation coefficient, R^2 , of 0.9983. The comparison between the model and the second set of experimental data is shown in

Figure 4.

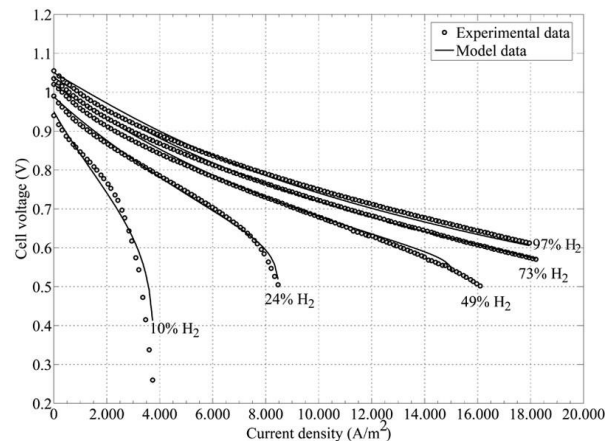


Figure 4. Comparison of experimental and model current-voltage curves from the second experiment. The lines are the model data and the circles are the experimental data.

Again the two sets of curves show a good agreement. The only exception occurs at 10% hydrogen concentration, where R^2 is 0.9547. The current-voltage curves for lower hydrogen

concentrations, in

Figure 4, show a characteristic "tail" where the voltage is rapidly reduced at increasing current-densities. This signifies the onset and the dominance of the concentration polarization, and is also the source of the greatest error. The error is caused by the concentration polarization which dominates almost completely at low hydrogen concentrations. This effect is difficult to model theoretically, because Equation (1.18) is only an approximation of the concentration polarization (Larminie and Dicks, 2004). This is a source of errors in the SOFC model, since the cell voltage is often determined at low hydrogen concentrations because of high fuel utilization.

5. Implementation in DNA

The SOFC model was implemented in FORTRAN77 and added to the existing DNA component library. In the implementation the cell area of the SOFC is assumed to be 144cm² (12cm × 12cm) instead of the 3.8cm² used in the calibration (Barfod, 2004). The area of future commercial SOFC will be as large as possible to obtain greater power, and the area of 3.8cm² only applies to an experimental SOFC. The implemented SOFC model was tested thoroughly, and has proved both robust and fast.

6. Model Sensitivity Analysis

The DNA model was subjected to a sensitivity analysis where the current-density was varied from 1 to 6000 A/m² at temperatures from 650°C to 800°C. The inlet temperature was 600°C and the fuel utilization was 80%. The analysis was performed with a hydrogen-based fuel with a molar composition of 96% H₂, 3% H₂ and 1% CO₂ and a methane-based fuel consisting of 33% CH₄ and 67% H₂O. The CO₂ in the hydrogen-based fuel is required to make the chemical sub-model converge. The above fuel mixtures were chosen to simulate possible operating conditions for future SOFCs. The current-density was converted to mass flow using Equations (1.5) and (1.7) to enhance the differences between the two fuel compositions. The result of the analysis, in terms of electrical power and electrical efficiency, are shown in Figure 5 and Figure 6 respectively.

The hydrogen-based fuel results in the highest power output, because the chemical equilibrium in the methane-based fuel results in a lower H₂ concentration and thus a lower voltage. The power curves for the methane-based fuel are located to the right compared to the hydrogen-based fuel, because the high content of water dilutes the fuel and a higher mass flow required to obtain the same current-densities. For both types of fuels, an increased operating

temperature results increase the power output, except at low mass flows, where the power is slightly higher at the lowest temperatures.

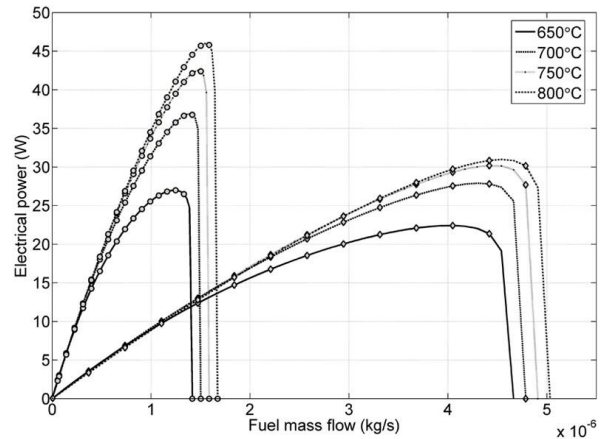


Figure 5. SOFC electrical power as a function of the mass flow. Results for hydrogen are marked with a "●" (left) and results for methane is marked with a "◆" (right).

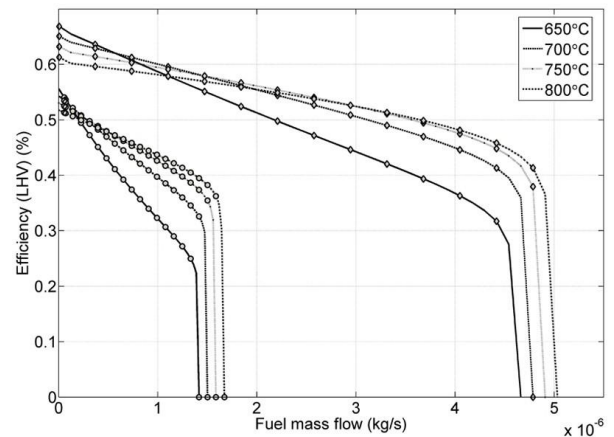


Figure 6. Electrical efficiency as a function of the mass flow. Results for hydrogen are marked with a "●" (left) and results for methane is marked with a "◆" (right).

The methane-based fuel results in the highest efficiency because this type of fuel has a much lower heating value (a factor of 5) than the hydrogen-based fuel, and because part of the heat released in the SOFC is reused to reform CH₄ to H₂. Like the electrical power the efficiency is highest at high temperatures at high mass flows and at low temperatures at low mass flows.

7. Discussion

The chemical sub-model of the SOFC can simulate both hydrogen and methane fueled SOFCs. However, the electrochemical sub-model is only completely valid for hydrogen fueled SOFCs because the expression for the binary diffusion coefficient was derived from a hydrogen/water/nitrogen fuel mixture. However, research has shown that the difference in

diffusion coefficients is relatively small, and the model is therefore assumed valid for both types of fuels (Barfod, 2004). Calibration of the general, theoretical polarization expressions, used in the electrochemical sub-model, gave a good agreement between the model and the experimental data. This was expected since, in essence, a fitted function is compared to the data used for the fitting. The calibration reduces the generality of the electrochemical sub-model which cannot be expected to model other SOFC accurately, because it is coupled to a specific cell. However, the only calibration specific parameters are the charge transfer coefficient, the exchange current-density, the B parameter and the binary diffusion constant. The described approach is therefore general and may be applied to all SOFCs. The cell voltage is evaluated using an average current-density, but the current-density changes over the cell with the minimum at the cell outlet (Sorrentino et al., 2004). Thus the operating voltage is underestimated as the polarizations increase with the current-density. This results in an error in the evaluated electrical power. The magnitude of the error is unknown, but assumed to be negligible.

8. Conclusion

A zero-dimensional model of a SOFC was developed for energy system simulation. The model accounts for the oxidation of hydrogen, the reforming of methane and the water-gas shift reaction using a flexible equilibrium model. The phenomenological electrochemical sub-model accounts for the offset, activation, Ohmic and concentration polarizations and was calibrated with experimental data. This approach resulted in a good agreement between the model and the experimental data. The SOFC model can be used to obtain reliable results, for SOFC behavior in the temperature range of 650°C to 800°C. The model was implemented in the DNA software, which was developed specifically for energy system simulation. The result is an accurate and flexible tool suitable for simulation of many types of SOFC-based energy systems.

Acknowledgements

The authors wish to thank Professor Michael J. Moran from Ohio State University, Jens Paalsson and Jens Nielsen from Haldor Topsøe A/S and Rasmus Barfod from Risø National Laboratory.

Nomenclature

A	Cell area (m ²)
B	Constant (-)
D	Diffusion coefficient (m ² s ⁻¹)
E	Electric potential (V)
F	Faraday's constant (Cmole ⁻¹)

i_{an}	Cathode limiting current (Am ⁻²)
i_{ca}	Anode limiting current (Am ⁻²)
i_d	Current density (Am ⁻²)
i_0	Exchange current-density (Am ⁻²)
L	SOFC length (m)
l	Length/thickness (m)
\dot{n}	Molar flow (mole ⁻¹)
P	Pressure (bar)
p	Partial pressure (bar)
R	Universal gas constant (kJkmole ⁻¹ K ⁻¹)
\dot{r}	Molar reaction rate (mole ⁻¹)
T	Temperature (K)
U_f	Utilization (-)
W	Electrical power (kW)
y	Molar concentration (-)
α	Charge transfer coefficient (-)
β	Pre-exponential factor (Am ⁻²)
ΔG^0	Gibbs energy (Jmole ⁻¹)
ΔV	Polarization (V)
ε	Porosity (-)
θ	Temperature (°C)
σ	Conductance. (Ω^{-1} m ⁻¹)
τ	Tortuosity factor (-)

Sub/Superscripts

0	Standard
a	Air
act	Activation
an	Anode
bin	Binary
ca	Cathode
con	Concentration
eff	Effective
el	Electrolyte
f	Fuel
H ₂	Hydrogen
in	Inlet
Nernst	Nernst potential
off	Offset polarization
Ohm	Ohmic polarization
out	Outlet
ox	Oxidation of hydrogen
ref	Reference

References

- Barfod, R., 2004, Personal communication with R. Barfod from Risø National Laboratories.
- Bove, R., Lunghi, P. and Sammes, N. M., 2005, SOFC mathematic model for systems simulations - Part 2: definition of an analytical model, *International Journal of Hydrogen Energy*, Vol. 30, No. 2, pp. 189-200.
- Braun, R., 2002, Optimal Design and Operation of Solid Oxide Fuel cell Systems for Small-scale Stationary Applications (PhD Thesis), University of Wisconsin-Madison.
- Chick, L. A., Williford, R. E., Stevenson, J. W., Windisch Jr., C. F. and Simner, S. P., 2003,

- Experimentally-calibrated spreadsheet based SOFC unit-cell performance, obtained from the Pacific Northwest National Laboratory.
- Costamagna, P., Magistri, L. and Massardo, A. F., 2001, Design and part-load performance of a hybrid system based on a solid oxide fuel cell reactor and a micro gas turbine, *Journal of Power Sources*, Vol. 96, No. 2, pp. 352-368.
- Costamagna, P., Selimovic, A., DelBorghi, M. and Agnew, G., 2004, Electrochemical model of the integrated planar solid oxide fuel cell (IP-SOFC), *Chemical Engineering Journal*, Vol. 102, No. 1, pp. 61-69.
- EG&G Technical Services, 2004, *Fuel Cell Handbook 7th Ed.*, U.S. Department of Energy.
- Elmegaard, B., 1999, Simulation of boiler dynamics - Development, Evaluation and Application of a General Energy System Simulation Tool (PhD Thesis), Technical University of Denmark.
- Henriksen, P. V., 2006, Personal communication with P. V. Henriksen from Risø National Laboratories.
- Iwata, M., Hikosaka, T., Morita, M., Iwanari, T., Ito, K., Onda, K., Esaki, Y., Sakaki, Y. and Nagata, S., 2000, Performance analysis of planar-type unit SOFC considering current and temperature distributions, *Solid State Ionics*, Vol. 132, No. 3-4, pp. 297-308.
- Keegan, K., Khaleel, M., Chick, L. A., Recknagle, K., Simner, S. and Deibler, J., 2002, Analysis of a Planar Solid Oxide Fuel Cell Based Automotive Auxiliary Power Unit, *SAE Technical Paper Series No. 2002-01-0413*.
- Larminie, J. and Dicks, A., 2004, *Fuel Cell Systems Explained Second Ed.*, John Wiley & Sons Inc., Chichester.
- Lienhard IV, H. J. and Lienhard V, H. J., 2004, *A heat transfer handbook 3rd Ed.*, Phlogiston Press, Cambridge.
- Massardo, A. F. and Lubelli, F., 2000, Internal reforming solid oxide fuel cell-gas turbine combined cycles (IRSOFC-GT): Part A - Cell model and cycle thermodynamic analysis, *Journal of Engineering for Gas Turbines and Power-Transactions of the Asme*, Vol. 122, No. 1, pp. 27-35.
- Petersen, T. F., 2004, Mathematical Model of a Solid Oxide Fuel Cell and Simulations of Hybrid Power Plants (MSc Thesis), Technical University of Denmark.
- Singhal, S. C. and Kendall, K., 2003, *High Temperature Solid Oxide Fuel Cells - Fundamentals, Design and Applications*, Elsevier Ltd., Oxford.
- Sorrentino, M., Mandourah, A., Petersen, T. F., Guezennec, Y., Moran, M. J. and Rizzoni, G., 2004, *Proceedings of the 2004 International Mechanical Engineering Congress and R & D Expo*, A 1-D model for the simulation of planar Solid Oxide Fuel Cells.